

# **Application of the discrete ordinates method to grey media in complex geometries using unstructured meshes**

by **D. JOSEPH\***, **P.J. COELHO\*\***, **B. CUENOT<sup>†</sup>**, **M. EL HAFI\***

\* *École des Mines d'Albi Carmaux, Campus Jarlard, route de Teillet, Albi, France, joseph@enstimac.fr and elhafi@enstimac.fr*

\*\* *Instituto Superior Técnico, Mechanical Engineering Department, Av. Rovisco Pais, 1049-001 Lisboa, Portugal, coelho@navier.ist.utl.pt*

<sup>†</sup> *C.E.R.F.A.C.S. 42, Av. Gaspard Coriolis, Toulouse, France, cuenot@cerfacs.fr*

## **Abstract**

A structured radiative heat transfer code based on the standard discrete ordinates method has been extended to unstructured meshes in order to be coupled with a CFD code. The code has been specially written for unstructured grids using tetrahedral cells, by trying to avoid complex adaptations that are time consuming. The mesh influence is studied for different cases. Results are compared with those obtained with an accurate method (ray tracing).

## **1 Introduction**

In Computational Fluid Dynamics (CFD), the coupling between radiative heat transfer and combustion is based on the solution of the energy equation. The heat source term due to radiation is evaluated by taking into account the temperature and radiating species concentrations profiles, which are obtained from the solution of the aerothermochemistry equations. Among all the numerical methods developed to calculate the radiative heat transfer, the Finite Volume Method (FVM) and the Discrete Ordinates Method (DOM) offer a good compromise between accuracy and computational requirements. These two methods have been widely used to solve radiative transfer problems in structured three-dimensional geometries using Cartesian or cylindrical coordinates. In particular, the DOM, described by Chandrasekar in 1950 [1], has been deeply studied by Lathrop and Carlson in 60-70's [2] and by Truelove, Fiveland and Jamaluddin in the 80's [3, 4, 5, 6, 7]. Significant improvements have been achieved in the last decade aiming at the reduction of the ray effects and false scattering, more accurate quadratures and the extension to complex geometries [8, 9, 10]. Nevertheless, the coupling between radiative transfer and other physical phenomena, such as combustion and fluid flow at high temperatures, requires the solution of the radiative transfer equation using the same grid employed to solve the other governing equations. Unstructured grids are often used in CFD owing to their geometrical flexibility. In this way, a lot of work has been developed during the last decade to apply the FVM to non-orthogonal structured grids and unstructured grids in three-dimensional enclosures [11, 12, 13, 14, 15]. For the DOM application, Sakami and co-workers proposed an accurate but complex method for the spatial discretization by taking into account the exponential extinction [16, 17, 18]. Liu et al. have used the "step" scheme, equivalent of the "upwind" scheme in CFD [14]. A computer code using unstructured meshes and based on the modelling of radiative transfer using DOM, as well as accounting for non-grey gas radiation, has been developed aiming at a future coupling with a combustion code available at the C.E.R.F.A.C.S. in Toulouse. In this work, this radiative code is described and applied to several test cases for validation purposes. The results are compared with accurate solutions available in

the literature, and obtained using other methods, which may be more accurate, but also too time consuming for industrial applications, such as the ray tracing method.

## 2 Radiative Transfer Equation (RTE)

### 2.1 Mathematical formulation

Considering an absorbing-emitting and non-scattering grey medium, the variation of the radiative intensity along a line of sight can be written as:

$$\frac{dI(\vec{s})}{ds} = \kappa I_b - \kappa I(\vec{s}) \quad (1)$$

where  $I(\vec{s})$  is the radiative intensity,  $I_b$  the radiative intensity of the blackbody, and  $\kappa$  the absorption coefficient. Boundary conditions for diffuse surfaces are taken from the relation giving the intensity leaving the wall  $I_w$  as a function of the blackbody intensity of the wall  $I_{b,w}$  and of the incident radiative intensity:

$$I_w(\vec{s}) = \epsilon_w I_{b,w} + \frac{\rho_w}{\pi} \int_{\vec{n} \cdot \vec{s}' < 0} I_w(\vec{s}') |\vec{n} \cdot \vec{s}'| d\Omega' = \epsilon_w I_{b,w} + \frac{\rho_w}{\pi} H \quad (2)$$

where  $\epsilon_w$  is the wall emissivity,  $\rho_w$  the wall reflectivity,  $H$  the irradiation,  $\vec{n}$  the unit vector normal to the wall and  $\vec{s}$  the direction of propagation of the incident radiation confined within a solid angle  $d\Omega$ .

### 2.2 DOM for unstructured grids

The RTE is solved for every discrete direction  $\vec{s}_i$ . The integration of the radiative transfer equation over the volume  $V$  of an element limited by a surface  $\Sigma$ , and the application of the divergence theorem yields:

$$\int_{\Sigma} I \cdot \vec{s} \cdot \vec{n} d\Sigma = \int_V (\kappa I_b - \kappa I(\vec{s})) dV \quad (3)$$

The domain is discretized in tetrahedra which is the simplest three-dimensional control volume shape. Indeed, every other form constituting an hybrid mesh can be under-meshed by tetrahedra. Assuming that  $I_b$  and  $I(\vec{s})$  are constant over the volume and associated with the centre of the cell,  $P$ , and that the intensities  $I_j$  at the faces are constant over each face and associated with the center of the corresponding face, equation (3) is discretized as:

$$\sum_{j=1}^{N_{face}=4} I_j \cdot (\vec{s}_i \cdot \vec{n}_j) \cdot A_j = \kappa V (I_{b,P} - I_P) \quad (4)$$

where  $\vec{n}_j$  is the outer unit normal vector of the  $j$ th face whose area is  $A_j$ . The scalar product of the  $i$ th discrete direction vector with the normal vector of the  $j$ th face of the considered tetrahedron is denoted by  $D_{ij}$ :

$$D_{ij} = \vec{s}_i \cdot \vec{n}_j = \mu_i n_{xj} + \eta_i n_{yj} + \xi_i n_{zj} \quad (5)$$

In order to calculate the radiation intensities at the cell faces, Ströhle et al. [10] proposed a spatial differencing scheme based on the mean flux that can be very useful in the case of unstructured grids. This scheme relies on the following formulation:

$$I_P = \alpha \overline{I_{out}} + (1 - \alpha) \overline{I_{in}} \quad (6)$$

where  $\overline{I_{in}}$  and  $\overline{I_{out}}$  are cell face averaged intensities entering and leaving the control volume, respectively:

$$\overline{I_{in}} = \frac{\sum_{\substack{j \\ D_{ij} < 0}} D_{ij} A_j I_j}{\sum_{\substack{j \\ D_{ij} < 0}} D_{ij} A_j} \quad (7)$$

and

$$\overline{I_{out}} = \frac{\sum_{\substack{j \\ D_{ij} > 0}} D_{ij} A_j I_j}{\sum_{\substack{j \\ D_{ij} > 0}} D_{ij} A_j} \quad (8)$$

Substituting  $\overline{I_{in}}$  from equation (6) into equation (4) yields:

$$I_P = \frac{\alpha V \kappa I_b - \Theta \sum_{\substack{j \\ D_{ij} < 0}} D_{ij} A_j I_j}{\alpha \kappa V + \sum_{\substack{j \\ D_{ij} > 0}} D_{ij} A_j} \quad (9)$$

with:

$$\Theta = \alpha - (1 - \alpha) \frac{\sum_{\substack{j \\ D_{ij} > 0}} D_{ij} A_j}{\sum_{\substack{j \\ D_{ij} < 0}} D_{ij} A_j} \quad (10)$$

The case  $\alpha = 1$  corresponds to the step scheme. After calculation of  $I_P$  from equation (9), the radiation intensities at cell faces such that  $D_{ij} > 0$  are set equal to  $\overline{I_{out}}$ , obtained from equation (6).

The discretization of the boundary condition (equation (2)) is straightforward:

$$I_w = \epsilon_w I_{b,w} + \frac{1 - \epsilon_w}{\pi} \sum_{\vec{n} \cdot \vec{s}_i < 0} w_i I_i |\vec{n} \cdot \vec{s}_i| \quad (11)$$

The DOM is based on the discretization of the solid angle  $4\pi$  in a chosen number  $N_{dir}$  of discrete directions  $\vec{s}_i(\mu_i, \eta_i, \xi_i)$  associated with the respective weights  $w_i$ . In this way, different angular discretizations can be used, namely the polar/azimuthal discretization typical of the FVM, the  $S_N$  and the  $T_N$  quadratures, the last two being the most used in the DOM. The results presented below have only used the  $S_N$  quadratures.

The control volumes should be treated following a sweeping order such that the radiation intensities at upstream cell faces are known. An algorithm for the optimization of the sweeping order was implemented in the present work. A sweeping order optimization not only avoids too many iterations for the cases with scattering media and/or reflective walls geometries, but also avoids iteration in the case of black walled enclosures without scattering. This order depends on the discrete direction under consideration.

### 3 Results and discussion

Several simple test cases have been carried out to validate the code for different types of enclosures with transparent or grey media. Four of these test cases are presented here. The influence of the grid size and angular discretization was evaluated.

#### 3.1 Black walled rectangular enclosure

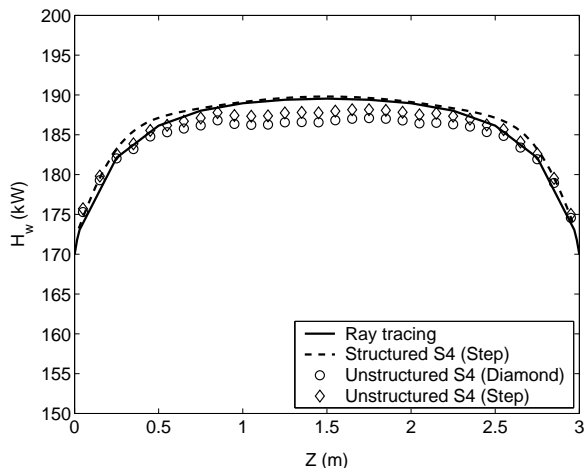
The first test case is made on a box-shaped furnace enclosure (1m x 1m x 3m). The walls are black at 1000°C and the medium is grey with  $\kappa = 0.1\text{m}^{-1}$  and at a temperature of 1500°C. Two unstructured grids have been tested. The coarse one has 3222 tetrahedra (case 1) and the fine one 20425 (case 2). The results are compared with those calculated using a cartesian grid with a 20x20x60 mesh and a reference solution calculated using ray tracing with 80000 rays (in this way, the results can be considered as numerically quasi-exact). The incident heat flux,  $H_w$ , along the centerline of the largest walls is shown in figure 1. The tests have been performed for three different  $S_N$  quadratures -  $S_4$ ,  $S_8$  and  $S_{12}$  - and two different spatial differencing schemes - diamond mean flux scheme ( $\alpha = 0.5$ ) and step scheme. The results obtained using an unstructured mesh are in good agreement with the reference solution regardless of the quadrature and the grid refinement. The spatial discretization scheme has a marginal influence on the accuracy of the results. Further calculations were performed using the unstructured fine mesh rotated by 45° around the z-axis (case 3, see figure 1). The  $S_8$  solution is significantly worse than in case 2, contrary to the other solutions. The reason for this is not clear, but may be due to the ray effect.

#### 3.2 L-shaped enclosure containing a grey medium

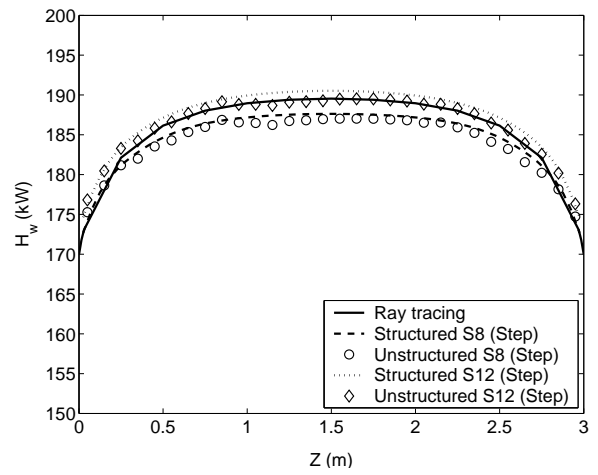
In this test, an L-shaped enclosure containing a grey emitting-absorbing medium at  $T = 1000\text{K}$  has been considered (see figure 2). The walls are black at  $T_w = 500\text{K}$ . The  $S_4$  angular quadrature is used and the number of cells is 17192. The results obtained for four different values of  $\kappa$  are presented in figure 2(c). The results obtained with the step scheme have been compared with those presented by Sakami et al. (DOM using an  $S_4$  quadrature with the exponential spatial discretization scheme applied to a grid comprising 2000 tetrahedra) [19] and by Malalasekera and James (Discrete Transfer Method applied to a non-orthogonal structured grid) [20]. The difference between the present results and those obtained in [19] and [20] is not large. The grid used here is fine, showing that a step scheme used with a fine mesh can give results similar to those of the exponential scheme, which is more accurate.

#### 3.3 Cylindrical enclosure with transparent medium

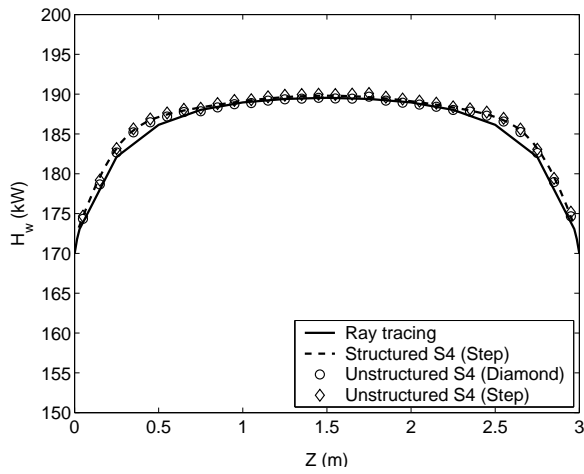
As a third test, a cylindrical black walled enclosure ( $h = 2\text{m}$  and  $r = 1\text{m}$ ) with a transparent medium is considered. The top and side walls are cold, while the bottom one is maintained at temperature  $T_w = 1000\text{K}$ . The unstructured grid has 2591 cells. The ray tracing method is em-



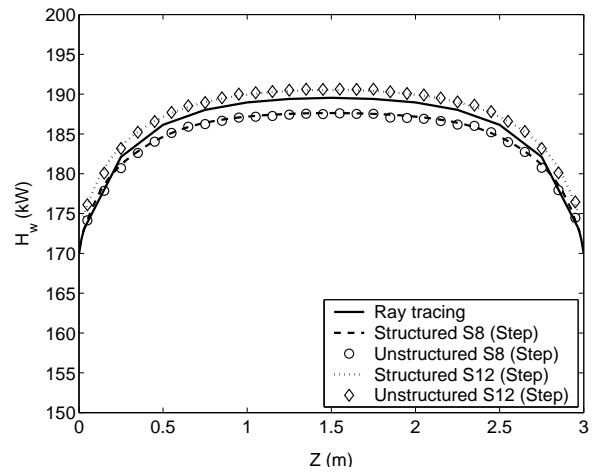
(a) Case 1: Coarse grid (number of control volumes = 3222 tetrahedra)



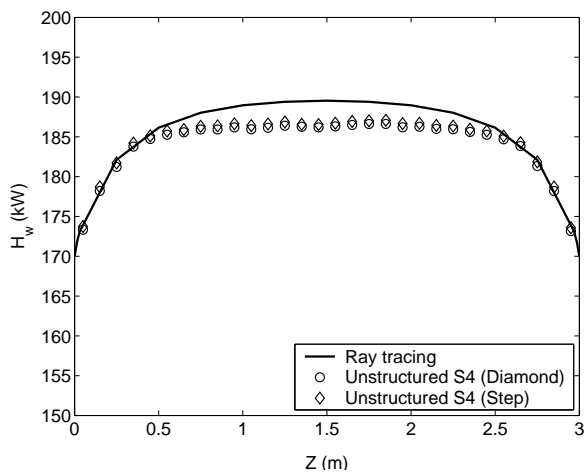
(b) Case 1: Coarse grid (number of control volumes = 3222 tetrahedra)



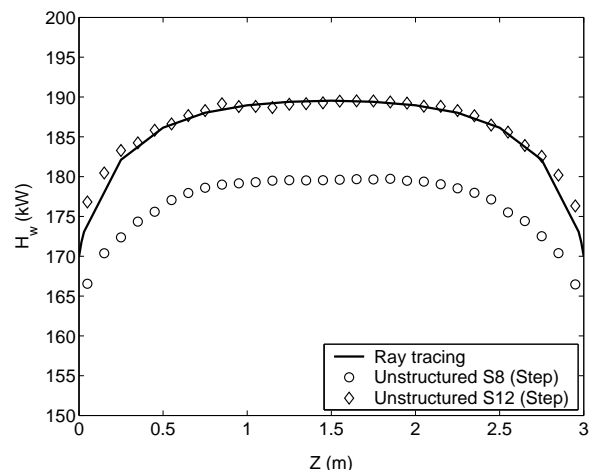
(c) Case 2 : Fine grid (number of control volumes = 20425 tetrahedra)



(d) Case 2 : Fine grid (number of control volumes = 20425 tetrahedra)

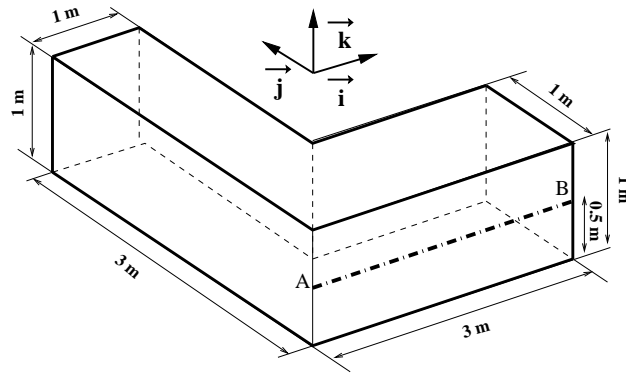


(e) Case 3 : Fine grid 45°-rotated (number of control volumes = 20425 tetrahedra)

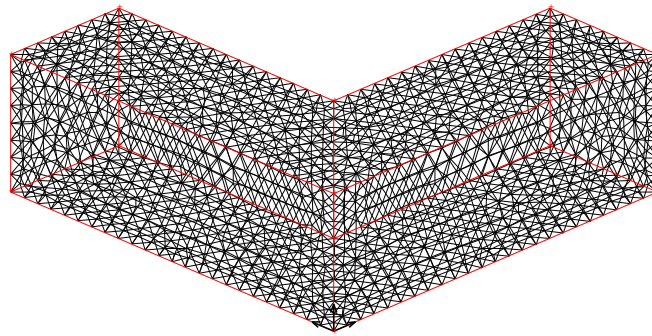


(f) Case 3 : Fine grid 45°-rotated (number of control volumes = 20425 tetrahedra)

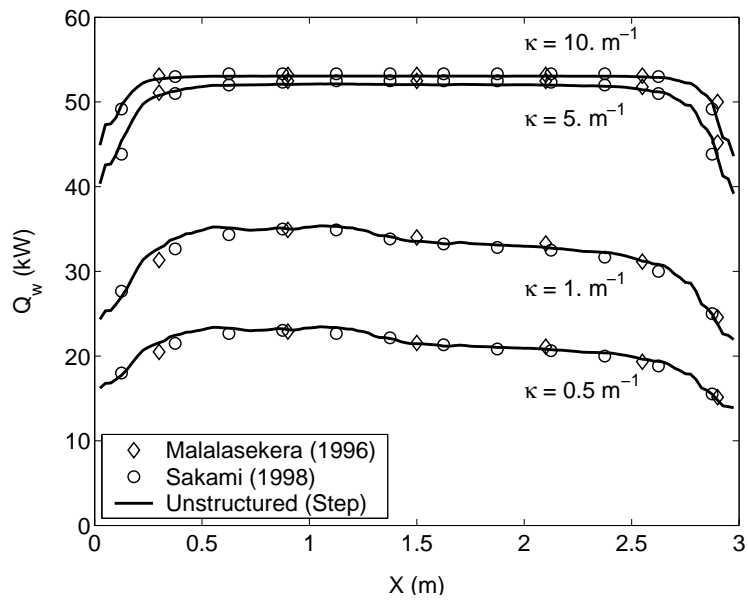
Figure 1: Black walled rectangular enclosure case



(a) The L-shaped geometry



(b) The L-shaped mesh : 17192 cells



(c) Radiative net heat flux at the wall along the line AB of the L-shaped enclosure case using the step scheme and the  $S_4$  quadrature with different values for  $\kappa$

Figure 2: The L-shaped enclosure case

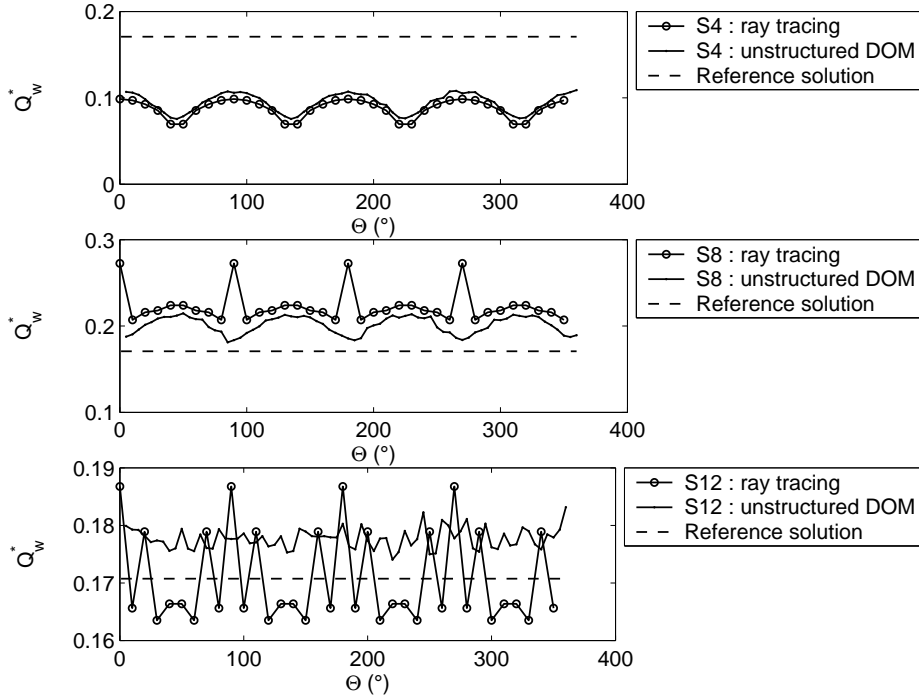


Figure 3: Non-dimensional net heat flux wall along the perimeter of the cylinder at midheight ( $z_o = 1\text{m}$ ): comparison ray tracing / unstructured DOM with the same angular quadrature

ployed with a small number of directions, namely the directions defined by the  $S_N$  quadratures (those of the quadrature set used in the DOM code). The results obtained using the ray tracing method are independent of the grid, allowing the decoupling of the ray effect due to the angular discretization from the mesh influence. Figure 3 shows the non-dimensional net heat flux normalized by the emissive power of the hot wall,  $Q_w^*$ , along the perimeter of the cylinder and at midheight ( $z_o = 1\text{m}$ ). The dashed line stands for the exact value, which must be the same along the perimeter. The ray tracing solution exhibits greater oscillations, which are caused by the ray effect. In the DOM, the ray effect is smoothed by the false scattering associated with the spatial discretization.

### 3.4 Cylindrical enclosure with participating grey medium

Finally, a cylinder ( $h = 3\text{m}$  and  $r = 0.5\text{m}$ ) containing a grey isothermal medium at  $T = 1200\text{K}$  is considered. The walls are at  $T_w = 300\text{K}$ . The radiative heat source  $S_r$  along the central axis of the cylinder and the radiative net heat flux  $Q_w$  at the side wall are obtained with the unstructured code using the step scheme and the  $S_8$  quadrature. The grid used in this test case is relatively coarse (2591 tetrahedra). Results are compared to those obtained with a ray tracing method using 320000 rays (figure 4). In this case of a homogeneous medium, the results of the ray tracing method are also grid independent. The DOM results are in good agreement with the ray tracing solution, regardless of the absorption coefficient of the medium. In the case of optically thin media, the peak of the net heat flux predicted by the DOM is about 10% lower than the ray tracing solution, but the two solutions become closer with the increase of  $\kappa$ . The radiative heat source predicted by the DOM is in excellent agreement with the ray tracing solution for  $\kappa = 0.1\text{m}^{-1}$ . The increase of the absorption coefficient of the medium yields also an increase of the radiative heat source. However, for optically thick media,  $\kappa = 10.\text{m}^{-1}$ , the radiative heat source decreases,

because most of the energy emitted by the medium is absorbed within a very short distance. In such a case, the relative difference between the DOM and ray tracing solutions is significant, since the radiative source approaches zero, but the absolute difference is still small.

## 4 Conclusion

A DOM code using unstructured grids has been developed. The code has been validated for transparent and grey media. The ray effect influence has been investigated and the compensation between ray effects and false scattering errors has been shown. The method used is relatively accurate. The introduction of an SNB-CK model into the code is in progress in order to take the spectral dependencies into account.

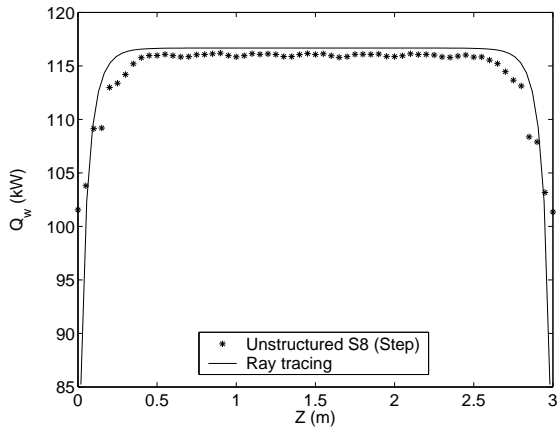
## Acknowledgements

The financial support of the European Commission in the framework of the TMR programme (RADIARE project, No. ERBFMRX-CT98-224) is gratefully acknowledged.

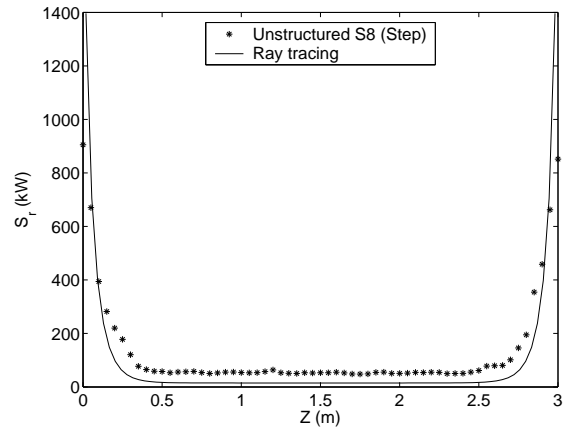
## References

- [1] S. Chandrasekhar. *Radiative transfer*. Clarendon Press, 1950.
- [2] B.G. Carlson and K.D. Lathrop. *Transport theory - The method of discrete ordinates*. in : Computing in reactor Physics, Ed. Gordon and Breach, 1968.
- [3] W.A. Fiveland. Three-dimensional radiative heat transfer solutions by the discrete-ordinates method. *J. Thermophysics*, 2(4):309–316, 1988.
- [4] W.A. Fiveland and A.S. Jamaluddin. Three-dimensional spectral radiative heat transfer solutions by the discrete-ordinates method. *J. Thermophysics*, 5(3):335–339, 1991.
- [5] W.A. Fiveland and J.P. Jessee. Comparison of discrete ordinates method formulations for radiative heat transfer in multidimensional geometries. *Journal of Thermophysics and Heat Transfer*, 9(1):47–54, 1995.
- [6] J.S. Truelove. Three-dimensional radiation in absorbing-emitting-scattering in using the discrete-ordinates approximation. *JQSRT*, 39:27–31, 1988.
- [7] A.S. Jamaluddin and P.J. Smith. Discrete-ordinates solution of radiation transfer equation in nonaxisymmetric cylindrical enclosures. *J. Thermophysics and Heat Transfer*, 6(2):242–245, 1992.
- [8] J.C. Chai, S.V. Patankar, and H.S. Lee. Evaluation of spatial differencing practices for the discrete-ordinates method. *J. Thermophysics and Heat Transfer*, 8(1):140–144, 1994.
- [9] C.P. Thurgood, A. Pollard, and H.A. Becker. The TN quadrature set for the discrete ordinates method. *Journal of Heat Transfer*, 117:1068–1070, 1995.
- [10] J. Ströhle, U. Schnell, and K.R.G. Hein. A mean flux discrete ordinates interpolation scheme for general coordinates. *3rd International Conference on Heat Transfer (Antalya)*, 2001.
- [11] G.D. Raithby and E.H. Chui. A Finite Volume Method for predicting a radiant heat transfer in enclosures with participating media. *Journal of Heat Transfer*, 112:415–423, 1990.
- [12] J.C. Chai, G. Parthasarathy, H.S. Lee, and S.V. Patankar. Finite volume radiative heat transfer procedure for irregular geometries. *Journal of Thermophysics and Heat Transfer*, 9(3):410–415, 1995.
- [13] J.Y. Murthy and S.R. Mathur. Finite Volume Method for radiative heat transfer using unstructured meshes. *Journal of thermophysics and heat transfer*, 12(3):313–321, 1998.

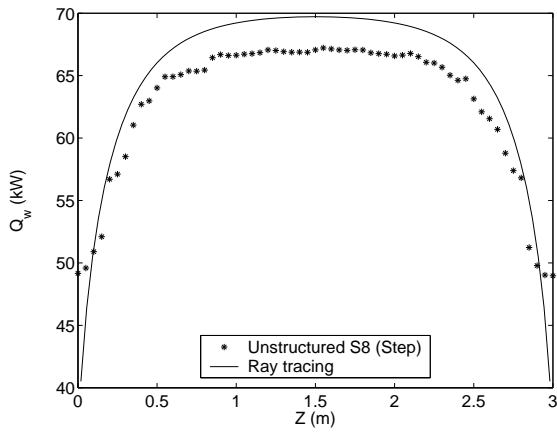




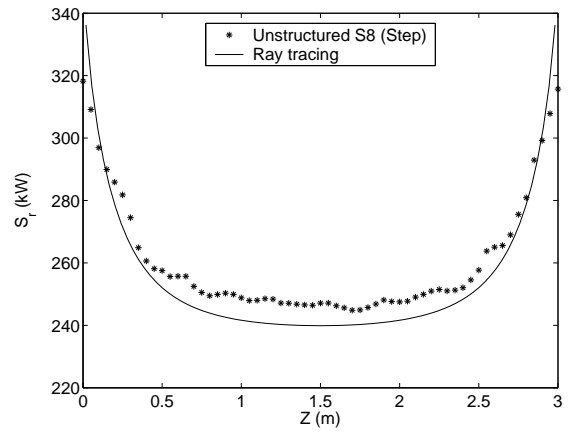
(a) Case 1:  $Q_w$  on the side wall for  $\kappa = 10.0m^{-1}$



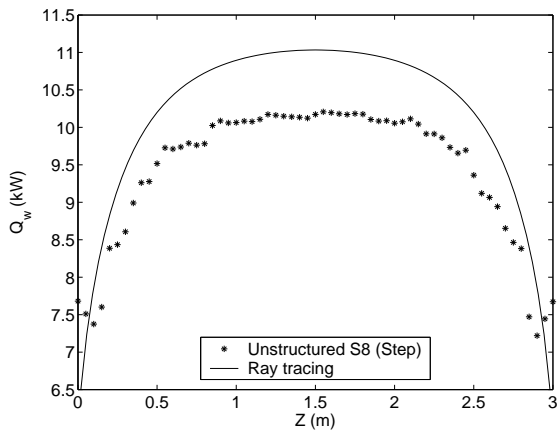
(b) Case 1:  $S_r$  on the side wall for  $\kappa = 10.0m^{-1}$



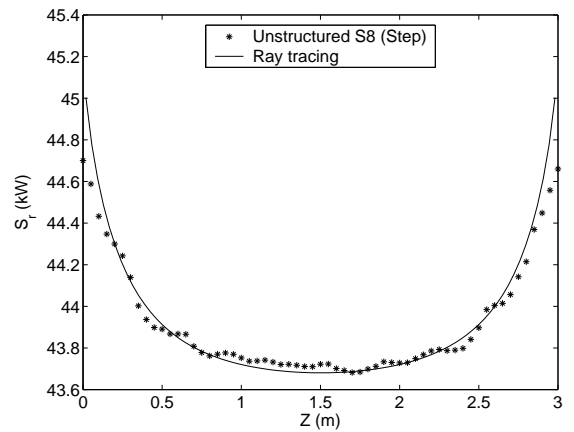
(c) Case 2 :  $Q_w$  on the side wall for  $\kappa = 1.0m^{-1}$



(d) Case 2 :  $S_r$  on the side wall for  $\kappa = 1.0m^{-1}$



(e) Case 3 :  $Q_w$  on the side wall for  $\kappa = 0.1m^{-1}$



(f) Case 3 :  $S_r$  on the side wall for  $\kappa = 0.1m^{-1}$

Figure 4: Cylindrical enclosure with participating grey medium : unstructured code using a coarse grid (2591 cells) compared to ray tracing.

- [14] J. Liu, H.M. Shang, Y.S. Chen, and T.S. Wang. Development of an unstructured radiation model applicable for two dimensional planar, axisymmetric and 3-dimensional geometries. *JQSRT*, 66:17–33, 2000.
- [15] J.P. Moder, G.N. Kumar, and J.C. Chai. An unstructured-grid radiative heat transfer module for the national combustion code. Technical Report AIAA-2000-0453, American Institute of Aeronautics and Astronautics, 2000.
- [16] M. Sakami, A. Charette, and V. LeDez. Application of the Discrete Ordinates Method to combined conductive and radiative heat transfer in a two-dimensional complex geometry. *JQSRT*, 56(4):517–533, 1996.
- [17] M. Sakami and A. Charette. A new differencing scheme for the Discrete Ordinates Method in complex geometries. *Revue générale de thermique*, 37:440–449, 1998.
- [18] M. Sakami and A. Charette. Application of a modified Discrete Ordinates Method to two-dimensional enclosures of irregular geometries. *JQSRT*, 64:275–298, 2000.
- [19] M. Sakami, A. Charette, and V. LeDez. Radiative heat transfer in 3-dimensional enclosures of complex geometry by using the discrete-ordinate method. *JQSRT*, 59(1/2):117–136, 1998.
- [20] W.M.G. Malalasekera and E.H. James. Radiative heat transfer calculations in three dimensional complex geometries. *Journal of Heat Transfer*, 118:225–228, 1996.